DOI: 10.1002/chem.200500031

Functionalized Nanodiamonds Part I. An Experimental Assessment of Diamantane and Computational Predictions for Higher Diamondoids

Andrey A. Fokin,*[a] Boryslav A. Tkachenko,[b] Pavel A. Gunchenko,[a]
Dmitriy V. Gusev,[a] and Peter R. Schreiner*[b]

Dedicated to Professor Paul von R. Schleyer for his outstanding contributions to the chemistry of diamondoids and on the occasion of his 75th Birthday

Abstract: The structures, strain energies, and enthalpies of formation of diamantane **1**, triamantane **2**, isomeric tetramantanes **3–5**, T_d-pentamantane **6**, and D_{3d}-hexamantane **7**, and the structures of their respective radicals, cations, as well as radical cations, were computed at the B3LYP/6-31G* level of theory. For the most symmetrical hydrocarbons, the relative strain (per carbon atom) decreases from the lower to the higher diamondoids. The relative stabilities of isomeric diamondoidyl radicals vary only within small limits, while the stabilities of the diamondoidyl cations increase with cage size and depend strongly on the geometric position of the charge. Positive charge located close to the geometrical center of the molecule is stabilized by 2–5 kcal mol^{-1}. In contrast, diamondoid radical cations preferentially form highly delocalized structures with elongated peripheral C−H bonds. The effective spin/charge delocalization lowers the ionization potentials of diamondoids significantly (down to 176.9 kcal mol^{-1} for **7**). The reactivity of **1** was extensively studied experimentally. Whereas reactions with carbon-centered radicals (Hal)$_3$C$^{\bullet}$ (Hal = halogen) lead to mixtures of all possible tertiary and secondary halodiamantanes, uncharged electrophiles (dimethyldioxirane, *m*-chloroperbenzoic acid, and CrO_2Cl_2) give much higher tertiary versus secondary selectivities. Medial bridgehead substitution dominates in the reactions with strong electrophiles (Br_2, 100% HNO_3), whereas with strong single-electron transfer (SET) acceptors (photoexcited 1,2,4,5-tetracyanobenzene) apical C^4−H bridgehead substitution is preferred. For diamondoids that form well-defined radical cations (such as **1** and **4–7**), exceptionally high selectivities are expected upon oxidation with outer-sphere SET reagents.

Keywords: cations · diamondoids · radicals · selective functionalization · single-electron transfer

Introduction

Diamondoids are defined as a group of cage hydrocarbons with carbon frameworks resembling the diamond lattice. The intensive development of the chemistry of cage compounds was initiated by Schleyer's discovery of a simple preparation of adamantane through the "stabilomeric" rearrangement of tetrahydrodicyclopentadiene catalyzed by Lewis acids.[1] Analogous thermodynamically controlled isomerizations of norbornene[2] or norbornadiene[3] dimers were used for the preparation of diamantane, the next representative diamondoid. Unfortunately, the "stabilomeric" approach is not efficient for the preparation of higher diamondoids (i.e., larger than tetramantane) because these possess multiple, energetically close, low-lying minima so that mixtures of isomers ensue. Hence, to date only triamantane[4] and C_{2h}-tetramantane have been prepared synthetically.[5,6] The synthetic inaccessibility of higher diamondoids is the main reason why the chemistry of these fascinating cage hydrocarbons is virtually undeveloped. The fact that dia-

---

[a] Prof. Dr. A. A. Fokin, Dr. P. A. Gunchenko, D. V. Gusev
Department of Organic Chemistry, Kiev Polytechnic Institute
pr. Pobedy 37, 03056 Kiev (Ukraine)
Fax: (+38) 044-241-7611
E-mail: aaf@xtf.ntu-kpi.kiev.ua

[b] Dr. B. A. Tkachenko, Prof. Dr. P. R. Schreiner
Institut für Organische Chemie, Justus Liebig University
Heinrich-Buff-Ring 58, 35392 Giessen (Germany)
Fax: (+49) 641-993-4309
E-mail: prs@org.chemie.uni-giessen.de

Supporting information for this article is available on the WWW under http://www.chemeurj.org/ or from the author.

mondoids (ca. 1–5 nm) bridge the nanometer-scaled size gap between molecular diamond-like structures (such as adamantane and diamantane, ca. 0.2–0.5 nm) and macromolecular small diamonds (ca. 1–100 nm), often referred to as "nanodiamonds",[7] make them particularly attractive for the preparation of pharmacologically active compounds (pronounced membrane activity[8] due to the high lipophilicity of the aliphatic core structure is expected, as for adamantane[9]), polymers with high rigidity,[10] and hybrid materials.[11]

As higher diamondoids are now accessible in sizeable quantities from crude oil,[12–14] the quest for their selective functionalization arises. It is clear that the large number of similarly reactive tertiary C–H bonds makes this a rather challenging task; the secondary positions are even more difficult to functionalize selectively due to their lower reactivity and reduced steric accessibility.

Many preparatively useful procedures for the functionalization of cage compounds are based on the reactions with electrophiles, radicals, and strong single-electron oxidizers.[15,16] The most useful are electrophilic oxidizers, which often react selectively with tertiary C–H bonds of cage hydrocarbons. These reactions are mechanistically neither radical[17] nor purely electrophilic in nature,[18] and instead proceed through H-coupled electron-transfer pathways.[19,20] As there is only one type of tertiary C–H bond in adamantane, it reacts selectively with neat Br_2,[21] ICl,[22] and 100 % HNO_3,[23] making many tertiary adamantane derivatives available in high preparative yields, even on industrial scale. Selective functionalization of diamantane with electrophiles gives medial tertiary C^1 derivatives; apical C^4 derivatives can only be obtained indirectly.[24] The chemistry of the higher diamondoids was explored only roughly as, for instance, triamantane already reacts with electrophiles with very low selectivities.[25]

The present paper aims at answering the key question: Which approaches are most useful for the selective preparation of functionalized diamondoids, that is, which reagents will allow the desired discrimination between the non-equivalent and similarly reactive tertiary C–H positions? Ionic, radical, and radical cationic pathways are considered in our experimental assessment of diamantane **1** and computational predictions for higher diamondoids.

Results and Discussion

Although both trivial and systematic[26] nomenclatures were proposed for diamondoids, we refer to the point group of the respective hydrocarbon to differentiate between the iso-

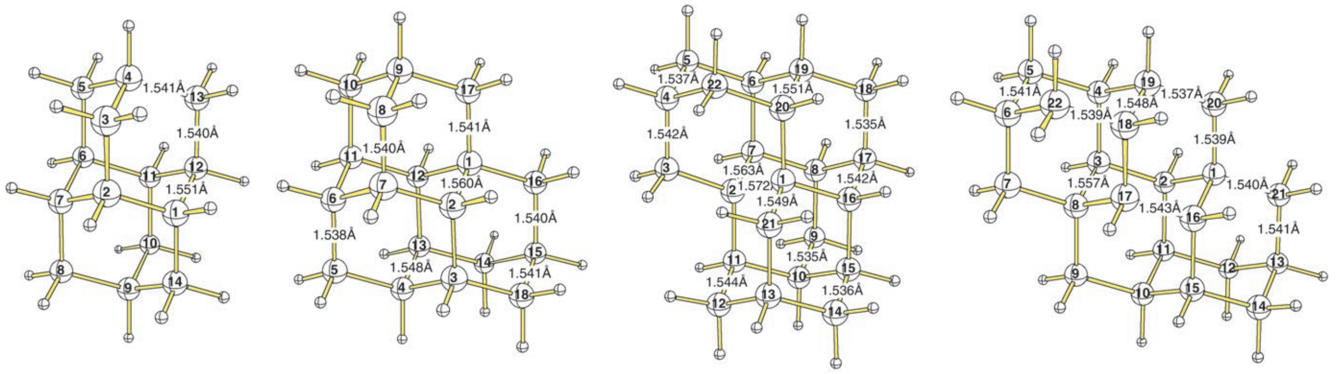

diamantane (**1**)
([1]diamantane,
congressane)

triamantane (**2**)
([12]triamantane)

C_2-tetramantane (**3**)
([123]tetramantane,
skew tetramantane)

C_{2h}-tetramantane (**4**)
([121]tetramantane,
anti-tetramantane)

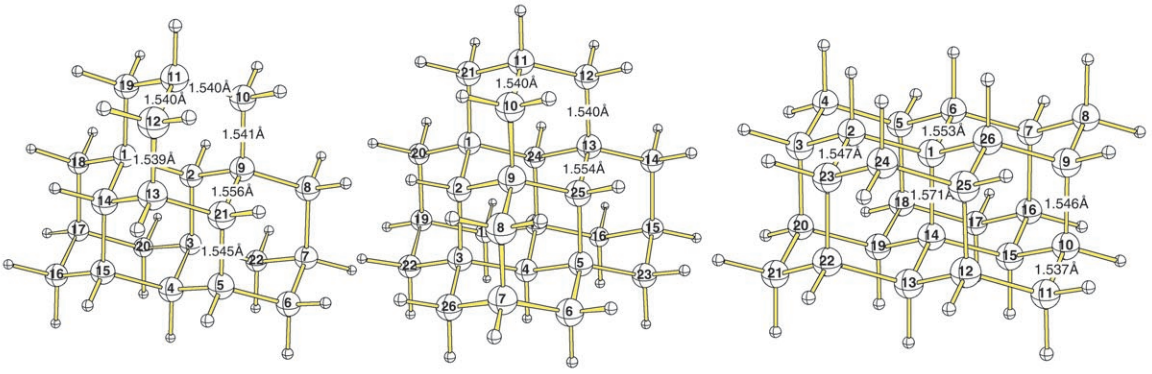

C_{3v}-tetramantane (**5**)
([1(2)3]tetramantane,
isotetramantane)

T_d-pentamantane (**6**)
([1(2,3)4]pentamanate)

D_{3d}-hexamantane (**7**)
(cyclohexamantane)

Figure 1. The B3LYP/6-31G* geometries of selected diamondoids with numbering of carbons.

mers more easily. Lower diamondoids involve diamantane (**1**, synthesized[2] and isolated from petroleum[27] in the 1960s); triamantane (**2**)[4] and C_{2h}-tetramantane (*anti*-tetramantane, **4**),[5] which were prepared synthetically and were also isolated from petroleum recently. C_2-Tetramantane (skew tetramantane, **3**), C_{3v}-tetramantane (isotetramantane, **5**), T_d-pentamantane (**6**),[12] and D_{3d}-hexamantane (cyclohexamantane, **7**)[13] are currently only available from petroleum. The B3LYP/6-31G* optimized geometries of these diamondoids with the numberings of the carbon cages are shown in Figure 1.

Strain energies: Strain energies are useful for predicting and understanding the reactivity of hydrocarbons.[28,29] Although diamondoids are comprised of almost perfectly tetrahedral geometries around their carbon atoms, they are, like the parent adamantane, not strain-free.[30] Among the various approaches to evaluate strain energies, those based on homodesmotic equations are most reliable due to the cancellation of systematic errors. We used Equations (1) and (2), which employ acyclic reference hydrocarbons, to give the strain energies directly. The B3LYP/6-31G* strain energies were evaluated by using Equation (1) for **1** ($n=2$, $k=18$, $l=6$, $m=8$, $p=0$), **2** ($n=3$, $k=24$, $l=7$, $m=10$, $p=1$), **3** and **4** ($n=4$, $k=30$, $l=8$, $m=12$, $p=2$), **5** ($n=4$, $k=30$, $l=9$, $m=10$, $p=3$), and **6** ($n=5$, $k=36$, $l=12$, $m=8$, $p=6$), and Equation (2) for **7**.

$$C_{4n+6}H_{4n+12} + k\,H_3CCH_3 = l\,H_3CCH_2CH_3 + m\,(CH_3)_3CH + p\,(CH_3)_4C \qquad (1)$$

$$C_{26}H_{30} + 37\,H_3CCH_3 = 6\,H_3CCH_2CH_3 + 18\,(CH_3)_3CH + 2\,(CH_3)_4C \qquad (2)$$

The calculated strain energy (E_{str}) of diamantane **1** (9.1 kcal mol^{-1}) is about 3 kcal mol^{-1} larger than that of adamantane.[29,30] However, the strain energy computed per carbon atom for both hydrocarbons is virtually identical (0.63 and 0.65 kcal mol^{-1}). The strain energy of **2** is only slightly higher (10.8 kcal mol^{-1}); the relative strain per carbon decreases slightly (0.60 kcal mol^{-1}). The strain energies of the C_{2h}-**4** (12.3 kcal mol^{-1}) and C_{3v}-**5** (11.5 kcal mol^{-1}) tetramantanes are very close (0.56 and 0.52 kcal mol^{-1} per carbon, respectively). The higher strain of C_2-**3** ($E_{str}=17.5$, 0.79 kcal mol^{-1} per carbon) arises from distortions of the central molecular unit, which displays an elongated C^1–C^2 bond (1.572 Å), while T_d-pentamantane (**6**) is almost strainless ($E_{str}=9.3$, 0.36 kcal mol^{-1} per carbon). Thus, in going from the lower to the higher diamondoids, the relative strain (per carbon atom) decreases, at least for the most symmetrical representatives. The geometry of D_{3d}-hexamantane (**7**) is distorted ($E_{str}=16.2$, 0.62 kcal mol^{-1} per carbon) at the central molecular unit where the C^1–C^{14} bond is elongated significantly (1.571 Å).

Enthalpies of formation: We computed the heats of formation (Δ_fH_{298}) by using the homodesmotic Equations (3)–(6). The Δ_fH_{298} computed for **1** from Equation (3) is −34.1 kcal mol^{-1}, in excellent agreement with the experimental value of -34.87 ± 0.58 kcal mol^{-1}.[31] For triamantane **2** ($n=3$), for instance, we applied Equation (4) ($l=6$, $k=m=o=r=1$, $p=2$), Equation (5) ($k=l=m=o=p=r=1$), and Equation (6) ($k=l=o=p=r=1$, $s=3$, $m=6$). The Δ_fH_{298} of **2** is -43.2 ± 1.8 kcal mol^{-1} [−44.4, −41.4, and −43.8 kcal mol^{-1} from Eqs. (4), (5), and (6), respectively]; the Δ_fH_{298} values of the higher diamondoids **3**–**7** are -47.0 ± 2.0, -52.0 ± 3.5, -54.7 ± 4.5, -64.7 ± 5.5, and -54.7 ± 5.2 kcal mol^{-1}, respectively.

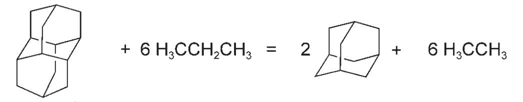

(3)

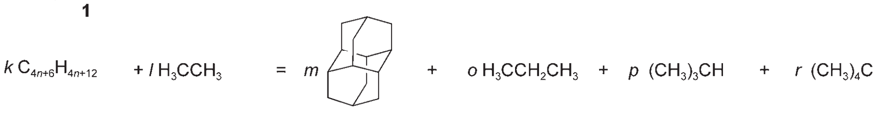

(4)

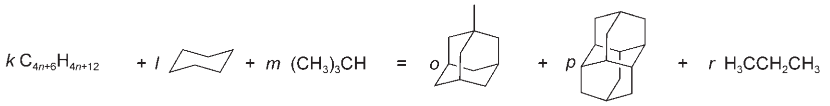

(5)

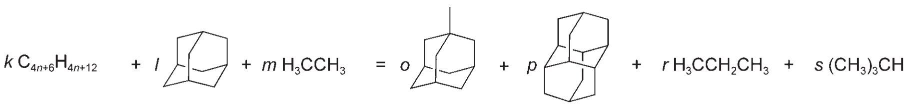

(6)

Diamondoidyl cations: Radical, ionic, and oxidative transformations are useful for the functionalization of cage compounds.[17] These are well developed for adamantane and its derivatives,[16,17,32] for which single-electron oxidations are usually the most selective.[33] In contrast to adamantane, higher diamondoids contain several non-equivalent tertiary C–H bonds: from two in **1** and **6** to six in **3**; this makes selective C–H substitutions rather difficult. It was shown previously that the positional selectivities for the C–H substitutions in cage compounds under ionic conditions correlate to a certain extent (exceptions are rare[34]) with the stability of the respective carbocations. We therefore calculated the relative stabilities (B3LYP/6-31G* ΔH_{298}, Figure 2) of diamondoidyl cations versus the 1-adamantyl cation (1-Ad$^+$) by using Equation (7). As expected, the relative stabilities increase continuously with cage size, and the penta- and hexamantyl cations (**6a**$^+$, **6b**$^+$, **7a**$^+$, and **7b**$^+$) are already

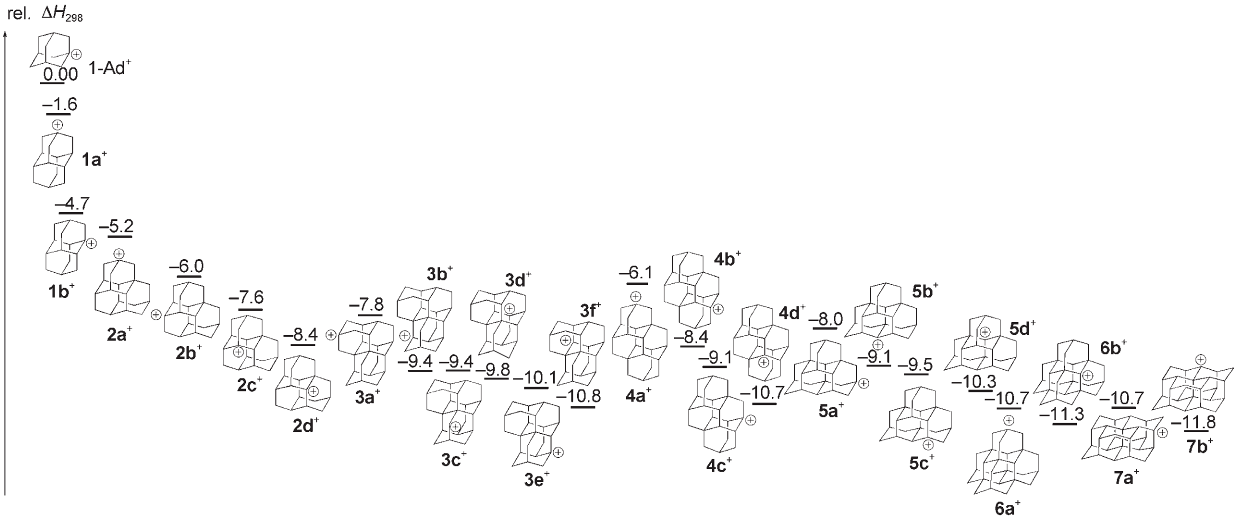

Figure 2. The B3LYP/6-31G* relative stabilities (ΔH_{298}, kcal mol^{-1}) of tertiary dimondoidyl cations versus the 1-adamantyl cation $C_{10}H_{15}^{+}$ defined by using Equation (7).

approximately 10 kcal mol^{-1} more stable than 1-Ad^{+} (Figure 2).

$$\text{1-Ad}^{+} + \text{diamondoid} \rightarrow \text{AdH} + \textit{tert}\text{-diamondoidyl}^{+} \qquad (7)$$

For isomeric cations, the relative stabilities depend directly on the position of the carbocationic center. Pronounced differences were found already for the two tertiary cations of **1** for which the 4-cation (**1a**$^{+}$) is approximately 3 kcal mol^{-1} less stable than the more delocalized 1-cation (**1b**$^{+}$). This delocalization is best visualized with the electrostatic potential (Figure 3) for which the blue and red colors indicate the areas of high positive and negative charge, respectively. The dispersion of charge is apparent from the lower intensities of the blue and red regions of the more stable medial cations. The distribution of the charge for C_{2h}-tetramantyl cations **4a**$^{+}$ and **4d**$^{+}$ is also shown in Figure 3.

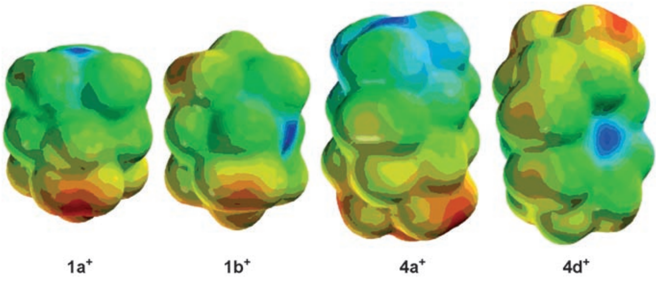

Figure 3. The electrostatic potentials of 4- and 1-diamantyl (**1a**$^{+}$ and **1b**$^{+}$) as well as those of the 6- and 2-C_{2h}-tetramantyl (**4a**$^{+}$ and **4d**$^{+}$) cations.

In general, placing the cationic carbon closer to the geometrical center of the molecule is favorable, and the peripheral cations are less stable; this is valid for all cations studied. For instance, for the least- and the most-stable C^{6}-(**4a**$^{+}$) and C^{2}-(**4d**$^{+}$) cations, respectively, the distances of the cation site to the geometric center are 3.309 and 1.282 Å, respectively. The increasing stabilities of tertiary cations enhance the reactivity of the higher diamondoids relative to adamantane under ionic conditions: triamantane reacts with bromine at 0 °C rapidly,[25] whereas the bromination of adamantane requires a longer reaction time or substantial heating.[21]

Diamondoidyl radicals: The correlation of the relative stabilities of hydrocarbon radicals with the selectivities in C–H substitution reactions is often crude because hydrogen-atom abstractions are mostly entropy-controlled.[17,35] We also computed all possible isomeric tertiary radicals derived from compounds **1**–**7**; the B3LYP/6-31G* ΔH_{298} values vary only in the range of 1 kcal mol^{-1}. Thus, free-radical substitutions in diamondoids are expected to depend on the structure of the abstracting radical (vide infra), rather than on the C–H bond strength. Nevertheless, pure radical reactions are not expected to be highly selective.

Diamondoid radical cations: Single-electron transfer (SET) oxidation reactions of hydrocarbons to radical cations require strong oxidants because the oxidation potentials of saturated hydrocarbons are rather high. As the HOMOs of cage hydrocarbons are typically highly delocalized, their radical cations also display pronounced spin/charge delocalizations over the entire cage. This lowers the ionization potentials (IPs) of cage hydrocarbons substantially (as a reference, the experimental vertical, IP$_{v}$, of adamantane is 9.28 eV (214.1 kcal mol^{-1}),[36] UB3LYP/6-31G* gives IP$_{v}$ = 214.0 kcal mol^{-1}, Figure 4). For larger cages the IPs decrease rapidly: The computed IP of diamantane **1** is 209.2 kcal mol^{-1} (experimental 8.93 eV, 206.0 kcal mol^{-1})[37] and only 182.3 kcal mol^{-1} for D_{3d}-hexamantane **7**.

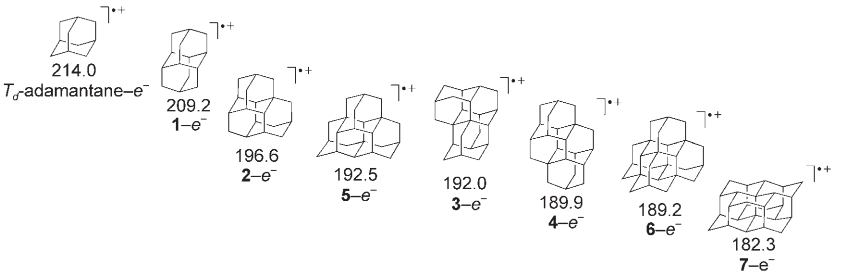

Figure 4. Vertical ionization potentials (IP_v, kcal mol^{-1}) of selected diamondoids at the UB3LYP/6-31G* level of theory computed on the B3LYP/6-31G* geometries of the neutral hydrocarbons.

Although the molecular structure of **1** belongs to the point group D_{3d}, this hydrocarbon is Jahn–Teller inactive because its HOMO is nondegenerate.[38] Thus, the relaxed radical cation of diamantane ($\mathbf{1}^{\cdot +}$) retains the symmetry of the parent molecule with the charge and spin being highly delocalized throughout the cage, which is comprised of six elongated co-parallel C–C bonds (1.588 Å, along the C_3 axis of the molecule) and two long apical tertiary C^4–H bonds (1.111 Å, Figures 5 and 6, vide infra). The opposite is found for diamantyl cations, for which the medial 1-cation ($\mathbf{1b}^+$, Figure 2) with elongated medial C–C bonds is more stable than the apical $\mathbf{1a}^+$. The radical cations usually undergo proton loss in solution from the position with the most elongated tertiary C–H bond. This predictable deprotonation usually produces the respective hydrocarbon radicals much more selectively than through radical hydrogen abstractions.[19,20,39–41] Thus, one expects different C–H bond selectivities for **1** under oxidative and nonoxidative conditions.

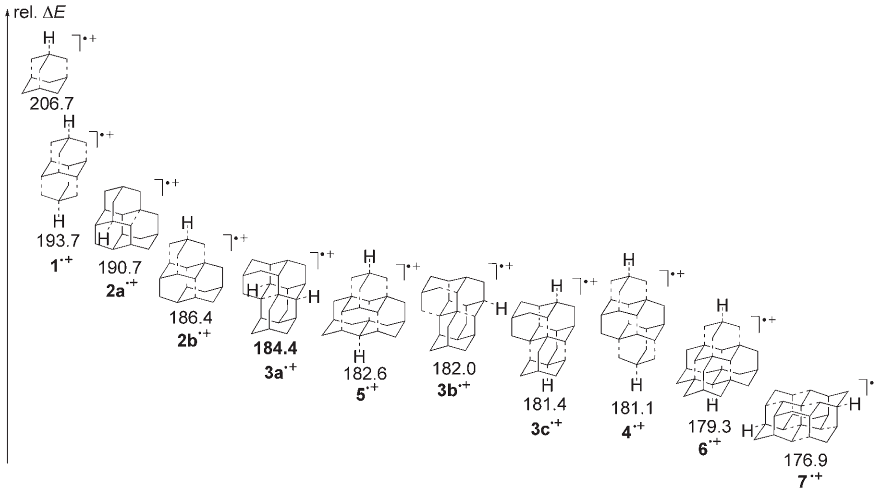

Figure 5. The B3LYP/6-31G* energies (ΔE, kcal mol^{-1}) of the relaxed diamondoid radical cations relative to the respective neutral hydrocarbons.

Triamantane (**2**) distorts to C_s symmetry after relaxation (the C_{2v} structure is not a minimum) either to $\mathbf{2a}^{\cdot +}$ or $\mathbf{2b}^{\cdot +}$, the latter being 4.3 kcal mol^{-1} more stable. Again, although the peripheral carbocation $\mathbf{2a}^+$ is the least stable among the tertiary tetramantyl cations, the radical cation with the elongated peripheral C–H bond, $\mathbf{2b}^{\cdot +}$, is more stable than $\mathbf{2a}^{\cdot +}$ due to the more pronounced delocalization of spin and charge in $\mathbf{2b}^{\cdot +}$.

There are three radical cation minima for C_2-tetramantane ($\mathbf{3a}^{\cdot +}$–$\mathbf{3c}^{\cdot +}$), with $\mathbf{3b}^{\cdot +}$ and $\mathbf{3c}^{\cdot +}$ being virtually identical in energy (the difference is only 0.6 kcal mol^{-1}). In contrast, **4** and **5** each give a single radical cation structure: the C_{2h}-tetramantane radical cation ($\mathbf{4}^{\cdot +}$) retains the symmetry of the neutral compound with two elongated apical tertiary C–H bonds and several elongated cage C–C bonds. This structure is the most stable among all the tetramantane radical cations computed. The HOMO of **5** is doubly degenerate and ionization/relaxation from the C_{3v} geometry leads to C_s-$\mathbf{5}^{\cdot +}$, which is even less stable than highly symmetrical C_{2h}-$\mathbf{4}^{\cdot +}$. Analogous to adamantane,[39] T_d-**6**, which has a triply degenerate HOMO, lowers its symmetry to give the C_{3v} structure $\mathbf{6}^{\cdot +}$. It should be pointed out, that in the case of hydrocarbons **1** and **4**–**7** different starting structures were used for the geometry optimizations and all these starting points converged to singular structures, shown in Figures 5 and 6.

Although **1** and **7** belong to the same D_{3d}-point group, different orbital orderings are observed: The HOMO of **7** is degenerate, and Jahn–Teller distortion upon ionization leads to the C_{2h} structure $\mathbf{7}^{\cdot +}$.

Despite the essential absence of strain, remarkably low adiabatic IPs were computed (177–184 kcal mol^{-1}) for the higher diamondoids. This makes SET oxidations of these hydrocarbons, even with conventional single-electron chemical oxidants (e.g., with tris(aryl)aminium salts[42]), valuable. As is seen from Figure 6, the structures of the diamondoid radical cations involve at least two significantly elongated (up to 1.111 Å) tertiary C–H bonds. The deprotonation from these positions is the most likely transformation of such species in solution. Thus, SET-induced functionalizations may even give a single tertiary C–H substitution product, especially if the elongated C–H bonds are identical chemically (as in the highly symmetrical radical cations $\mathbf{1}^{\cdot +}$, $\mathbf{4}^{\cdot +}$, and $\mathbf{7}^{\cdot +}$).

Reactivity: We consider **1**, which has two non-equivalent types of tertiary C–H bonds, as an experimental model for diamondoid functionalizations. Various reagents were exam-

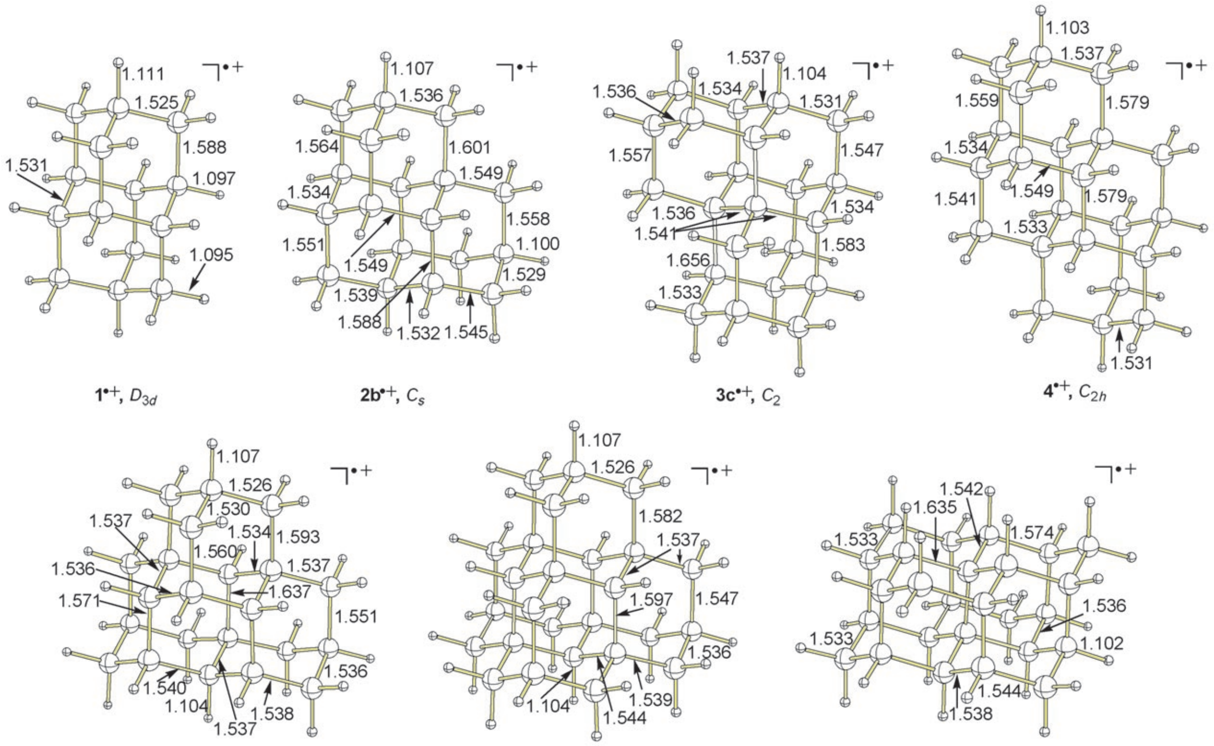

$1^{\bullet+}$, D_{3d} $2b^{\bullet+}$, C_s $3c^{\bullet+}$, C_2 $4^{\bullet+}$, C_{2h}

$5^{\bullet+}$, C_s $6^{\bullet+}$, C_{3v} $7^{\bullet+}$, C_{2h}

Figure 6. The B3LYP/6-31G* fully optimized geometries of the most favorable diamondoid radical cation structures.

ined to differentiate between the two tertiary positions. As the selectivities are usually higher under ionic conditions, a number of electrophilic reagents were used for the derivatizations of **1** (Scheme 1). Halogenations with electrophilic halogens gave the 1-bromo derivative **8** almost exclusively.[43] Under thermodynamically controlled conditions more stable 4-bromodiamantane (**9**) forms together with **8**.[43–45] The reaction with NO_2BF_4 in nitromethane gave a mixture of the 1- and 4-nitrodiamantanes **10** and **11**, respectively.[46] Nitration with nitronium trifluoromethane sulfonate, generated in situ from tetrabutylammonium nitrate and triflic anhydride, afforded nitro- or nitroxydiamantanes, depending on the solvent used (not shown); selectivities were not reported.[47] The oxidation of **1** with lead(IV) acetate[48] in CF_3COOH/CH_2Cl_2 led to a mixture of 1- and 4-hydroxydiamantanes (**12** and **13**, respectively) after aqueous workup. The direct preferential substitution of the apical position of **1** was achieved only by photooxidation with diacetyl and gave the 1- and 4-acetyldiamantanes **14** and **15**, respectively, in a ratio of approximately 1:5.[49]

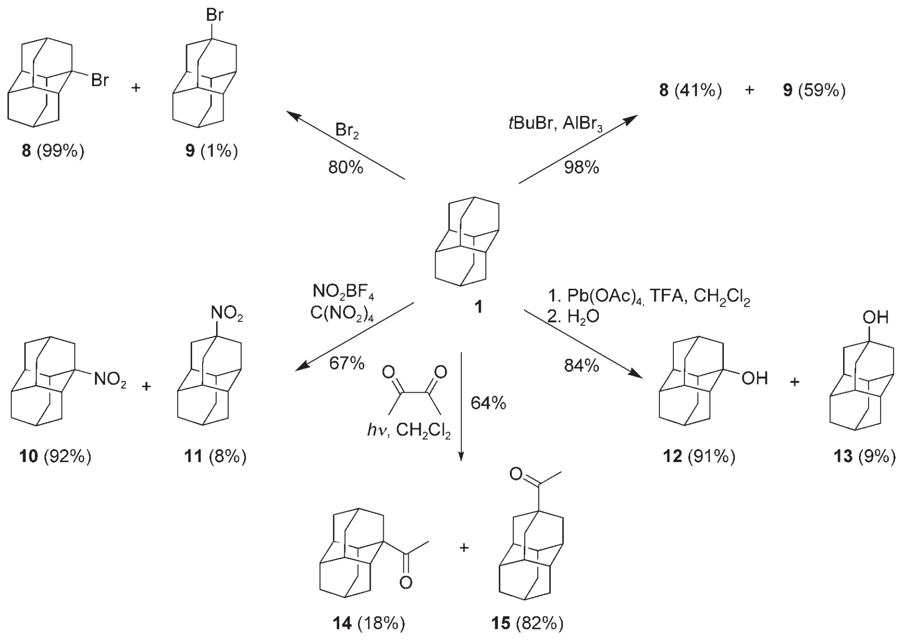

Scheme 1. The ratios and the preparative yields of the tertiary C–H substitution products described in the literature for **1** (TFA = trifluoroacetic acid).

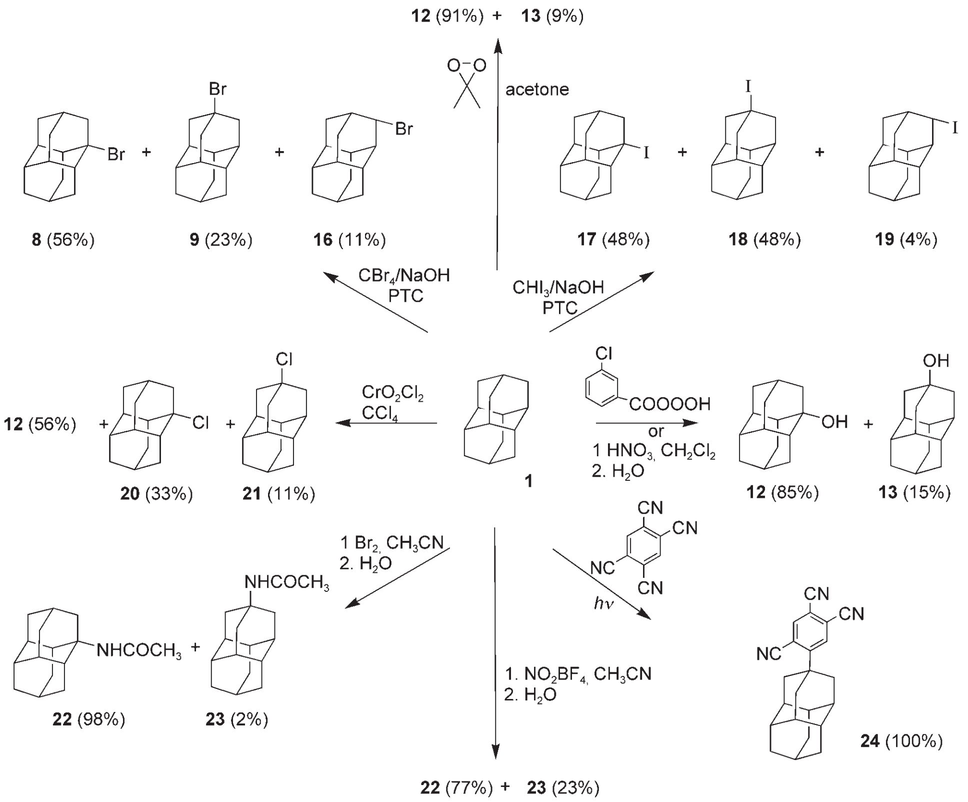

Scheme 2. The product ratios for the C–H substitutions of **1** with various reagents as elaborated in the present work (for preparative yields and full list of reagents including solvents used see the Experimental Section).

Thus, the selectivity problem for the two types of tertiary C–H bonds in **1** remains largely unsolved and there is also no practical way for the selective preparation of the structurally more attractive 4-substituted derivatives. In order to achieve higher selectivities for the apical C–H substitutions, we first turned our attention to carbon-centered radicals, which previously were shown to be most selective for radical tertiary versus secondary C–H substitutions of adamantane.[50] However, our computational assessment lowered our expectations regarding the selectivities for **1**. Indeed, reactions with the $Br_3C^{\bullet}$ as well as with the $I_3C^{\bullet}$ radicals generated under phase-transfer catalytic (PTC) conditions[51] from CBr_4 and HCI_3, respectively, gave mixtures of 1-, 3-, and 4-halodiamantanes (Scheme 2). The ratio of products is in full agreement with the B3LYP/6-31G* (3-21G* for I) data (Figure 7). For the reaction with $Br_3C^{\bullet}$, the lowest barrier (TS1, 14.8 kcal mol^{-1}, $\Delta G^{\ddagger}_{298}$) was computed for the hydrogen abstraction from the C^1–H position. The barriers for the abstraction from C^4–H and C^3–H (17.2 and 16.6 kcal mol^{-1} via TS2 and TS3, respectively) are higher. As a consequence, 1-bromodiamantane (**8**) is the main product of the bromination of **1** with $Br_3C^{\bullet}$ (Scheme 2). In contrast, the C^4–H position of **1** is the most reactive ($\Delta G^{\ddagger}_{298} = 26.3$ kcal mol^{-1}, TS5) towards $I_3C^{\bullet}$. The barriers for the abstraction from C^1–H and C^3–H are larger (29.1 and 28.9 kcal mol^{-1} via TS4 and TS6, respectively, Figure 7). The bulky $I_3C^{\bullet}$ radical favors the substitution at C^4–H because of substantial steric hindrance for C^1–H ab-

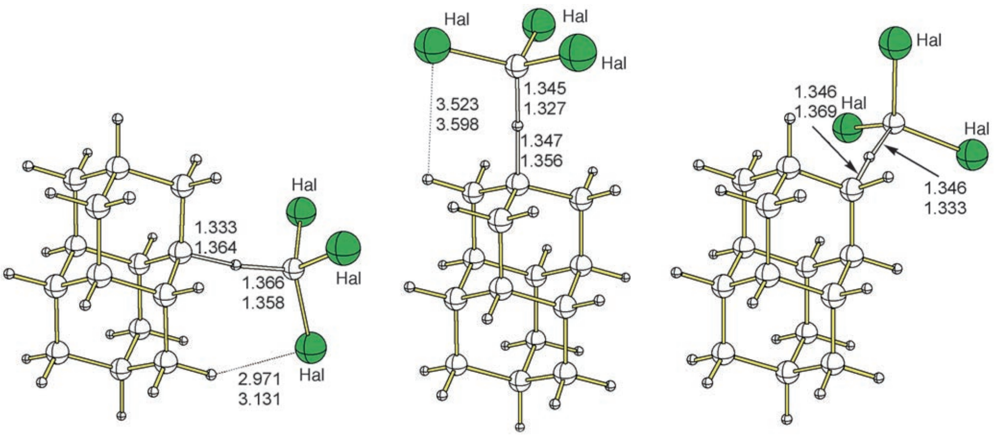

TS1 (Hal=Br) *0.0*
TS4 (Hal=I) *2.8*

TS2 (Hal=Br) *2.4*
TS5 (Hal=I) *0.0*

TS3 (Hal=Br) *1.8*
TS6 (Hal=I) *2.6*

Figure 7. The B3LYP/6-31G* (3-21G* for I) optimized geometries (selected interatomic distances in Å) for the transition structures for hydrogen abstractions from diamantane with the $Br_3C^{\bullet}$ (first entry) and $I_3C^{\bullet}$ (second entry) radicals and relative barriers $\Delta\Delta G^{\ddagger}_{298}$ (kcal mol^{-1}, italics).

straction (the crucial C···H distance in TS4 for the abstraction from this position is larger than that in TS5 for the C^4–H abstraction, Figure 7). Thus, the C^4–H substitution with the $I_3C^{\bullet}$ radical shows an inverse selectivity relative to the reactions of **1** with electrophiles, where C^1–H functionalizations dominate. However, radical reagents, even if they are as selective as $I_3C^{\bullet}$, are not very promising for the selective C–H functionalizations of diamondoids, because substantial amounts of secondary derivatives typically form.

Other types of reagents that play an important role in alkane chemistry are peroxo species like dioxiranes,[52] peracids,[53] as well as metal-oxo compounds.[54] The C–H activations with peracids and dioxiranes are believed to occur through concerted insertions,[55] that is, they are mechanistically different from radical abstractions. In contrast to the reactions with conventional radical abstractors, the hydrogen abstractions with metal-oxo reagents occur through highly polarized transition structures.[56] Despite these mechanistic differences, similar tertiary selectivities were observed in the reaction of **1** with dimethyl dioxirane, *m*-chloroperbenzoic acid, and with CrO_2Cl_2 for which C^1-substitution products form predominantly (Scheme 2); much higher tertiary versus secondary selectivities were observed.

The transformations of diamondoids with oxidizing electrophiles are usually more selective than with radical reagents or with uncharged electrophiles. For instance, the reaction with Br_2 in acetonitrile gave 1-acetaminodiamantane (**22**) almost exclusively (we found only traces of apical acetamide **23**). We have shown recently that the C–H substitutions of adamantane with electrophilic reagents (E) occur through H-coupled electron-transfer mechanisms[20] involving transition structures with linear C···H···E fragments. As nitronium electrophiles were previously successfully used for the functionalization of polycyclic hydrocarbons,[46,57] we used 100% nitric acid, in which nitronium nitrate $NO_2^+ NO_3^-$ is believed[58] to be responsible for the C–H activation. We first modeled this reaction computationally for the complex of NO_2^+ with one molecule of HNO_3 attacking the C^1–H (TS7) and C^4–H (TS8) positions of **1** (Figure 8).

The abstraction barriers are virtually identical ($\Delta G^{\ddagger}_{298}$ = 30.4 and 31.0 kcal mol^{-1}). Computations agree well with the ratio of products obtained earlier for the reaction of **1** with NO_2BF_4 in nitromethane,[46] as well as with our data on the reaction of **1** with NO_2BF_4 in acetonitrile, or with 100% HNO_3 in various solvents (Scheme 2), and the major substitution products derive from the statistically favored C^1–H position.

Strong single-electron acceptors, like photoexcited 1,2,4,5-tetracyanobenzene (TCB)[59] are able to oxidize alkanes.[19,33,40] The first step of these reactions involves outer-sphere electron transfer from the alkane to photoexcited TCB [Eq. (8)], followed by proton loss (in solution) from the alkane radical cation forming an alkyl radical [Eq. (9)] that couples with the aromatic reagent [Eq. (10)].

$$\text{Alk–H} + \text{ArCN}^* \rightarrow {}^{\cdot+}\text{Alk}\cdots\text{H}||\text{ArCN}^{\cdot-} \qquad (8)$$

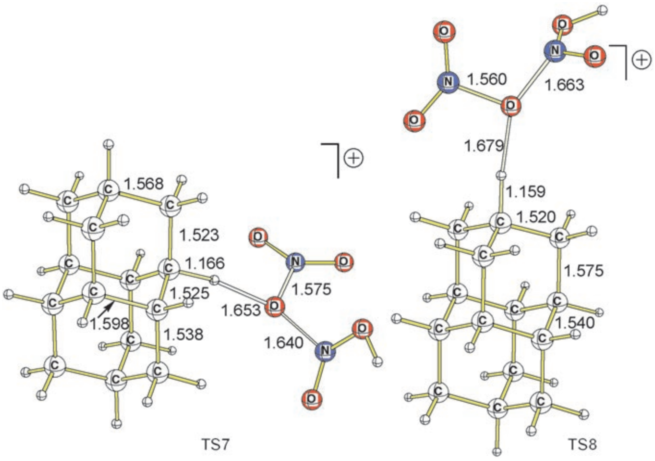

Figure 8. The B3LYP/6-31G* optimized geometries of the transition structures for the H-coupled electron transfer from diamantane to the NO_2^+···HNO_3 complex (selected interatomic distances in Å).

$$\text{Alk}\cdots\text{H}^{\cdot+} \rightarrow \text{Alk}^{\cdot} + \text{H}^+ \qquad (9)$$

$$\text{Alk}^{\cdot} + \text{ArCN}^{\cdot-} + \text{H}^+ \rightarrow \text{Alk–Ar} + \text{HCN} \qquad (10)$$

We found that oxidation of **1** with photoexcited TCB in acetonitrile gave a single adduct (**24**), that is, proton loss from the diamantane radical cation occurs exclusively from the C^4–H position. This agrees nicely with the computed structure of the diamantane radical cation $\mathbf{1}^{\cdot+}$ in which this C–H bond is substantially elongated relative to other C–H bonds (Figure 6). Thus, opposite selectivities are observed for the reactions of diamantane with electrophiles and outer-sphere SET oxidizers. The SET approach may also invert the selectivities in the functionalization of other higher diamondoids, which can subsequently be probed as novel nanostructural building blocks.

Conclusion

Naturally occurring diamondoids **2**–**7**, which are now available in large quantities, are expected to be more reactive than their parent molecules adamantane and diamantane (**1**). The selective functionalization of higher diamondoids still represents a formidable challenge because of the large number of similarly reactive tertiary C–H bonds.

The relative stabilities of diamondoidyl radicals vary only within small limits and conventional free-radical approaches lead to mixtures of all possible tertiary and even secondary diamondoid derivatives, as we have shown for **1** as a model. Uncharged electrophiles like peroxo or metal-oxo reagents behave similarly, but much higher tertiary versus secondary selectivities are observed for **1** and are expected for **2**–**7**.

Ionic transformations are more selective, as the differences in stabilities of isomeric tertiary diamondoidyl carbocations are quite pronounced. In the reactions with charged electrophiles, tertiary C–H bonds that are closer to the geometrical center of the molecule are most readily substituted. Varying the type of electrophile changes the selectivities only slightly, as found for **1** in the reactions with bromine and nitrogen-containing electrophiles.

Because the stabilization in the diamondoidyl cations is different from that in diamondoid radical cations, oxidative transformations involving outer-sphere electron transfer show inverted substitution selectivities relative to electrophilic reagents. This was found experimentally for **1**, which forms 1-substituted derivatives under electrophilic and 4-substituted derivatives under the SET oxidative conditions. For hydrocarbons that form a single radical cationic structure (such as **4**, **6**, and **7**) exceptionally high selectivities are expected upon oxidation with outer-sphere SET oxidizers. As the oxidation potentials of higher diamondoids are relatively low (ca. 170–180 kcal mol^{-1}), conventional chemical SET oxidants are useful for direct selective functionalization of higher diamondoids.

Experimental Section

Computational methods: Geometries were fully optimized at the B3LYP[60] level of theory with a 6-31G* basis set including frequency analyses to disclose the nature of all stationary points (Nimag = 0 for minima and 1 for transition structures). All computations were carried out by using the Gaussian 03 program package.[61] The reaction pathways along both directions from transition structures were verified by utilizing intrinsic reaction coordinates.[62] The *xyz* coordinates and the energies of the computed species are collected in the Supporting Information.

Bromination of 1 under phase-transfer catalytic (PTC) conditions: A mixture of **1** (0.66 g, 3.51 mmol), CBr_4 (4.5 g, 13.5 mmol), 50% aqueous NaOH (15 mL), Bu_4NBr (75 mg, 0.23 mmol), and CH_2Cl_2 (15 mL) was stirred at room temperature for 24 h, diluted with water (50 mL), and extracted with CH_2Cl_2 (3×15 mL). The combined extracts were washed with water and dried over Na_2SO_4; excess solvent was removed in vacuo. The residue was analyzed by GC–MS and showed conversion of approximately 95%; 1-bromodiamantane (**8**), 4-bromodiamantane (**9**), and 3-bromodiamantane (**16**) formed in a ratio of 56:23:11, respectively. The reaction mixture was separated by column chromatography (pentane as eluent) which gave **8** (366 mg, 39.2%), **9** (92 mg, 9.8%), and **16** (18 mg, 2%), with spectral data identical to literature values.[63,64]

Iodination of 1 under PTC conditions: A mixture of **1** (300 mg, 1.59 mmol), CHI_3 (1.4 g, 3.56 mmol), solid NaOH (3.5 g), and CH_2Cl_2 (10 mL) was stirred at room temperature for 48 h, diluted with water (30 mL), and extracted with CH_2Cl_2 (3×10 mL). The combined extracts were washed with an aqueous $NaHSO_3$ solution and water, and dried over Na_2SO_4; excess solvents were removed in vacuo. The residue was analyzed by GC–MS and showed conversion of approximately 75%; 1-iododiamantane (**17**), 4-iododiamantane (**18**), and 3-iododiamantane (**19**) formed in a ratio of 12:12:1, respectively. MS (70 eV): *m*/*z* (%) for **17**: 187 (100), 159 (3), 145 (8), 131 (11), 117 (6), 105 (10), 91 (18), 79 (21), 67 (7), 53 (4); MS (70 eV): *m*/*z* (%) for **18**: 187 (100), 159 (3), 145 (8), 131 (11), 117 (8), 105 (12), 91 (21), 79 (15), 67 (9), 53 (4); MS (70 eV): *m*/*z* (%) for **19**: 187 (100), 159 (7), 145 (6), 131 (10), 117 (6), 105 (7), 91 (21), 77 (18), 67 (15), 53 (9). The reaction mixture was separated by column chromatography (pentane as eluent), which gave a pure sample of 1-iododiamantane **17** (195 mg, 39%) and a mixture of **18** and **19** (137 mg, 27%). The ^{13}C NMR spectra of **17** and **18** were identical to literature data.[63] 3-Iododiamantane (**19**): ^{13}C NMR (75 MHz, $CDCl_3$, 25°C, TMS): δ = 25.7, 33.2, 34.0, 35.3, 35.8, 36.3, 37.3, 37.5, 37.7, 38.0, 39.2, 40.5, 46.7, 53.0 ppm.

Oxidation of 1 with HNO_3 in CH_2Cl_2: Compound **1** (2.8 g, 14.9 mmol), CH_2Cl_2 (25 mL), and 100% HNO_3 (3 mL, 71 mmol) were mixed at 0°C, stirred for 20 min at 0°C, and then 40 min at room temperature, and then diluted with water (14 mL). CH_2Cl_2 was then removed and the reaction mixture was refluxed for 1.5 h. A 17:3 ratio of 1-hydroxydiamantane (**12**)/4-hydroxydiamantane (**13**) was indicated by GC–MS (conversion ca. 95%). Column chromatography on silica gel (eluent of pentane/diethyl ether = 4:1) gave **1** (130 mg, 0.7 mmol), 1-hydroxydiamantane (**12**: 2.5 g, 82%), and 4-hydroxydiamantane (**13**: 0.4 g, 13%), with ^{1}H and ^{13}C NMR spectra identical to literature data.[45,64]

Oxidation of 1 with dimethyl dioxirane: A 0.1 M solution of dimethyl dioxirane (18 mL, 1.8 mmol) was added to a solution of **1** (200 mg, 1.06 mmol) in acetone (20 mL) under stirring at room temperature. The reaction mixture was analyzed by GC–MS after 24 h and was found to contain unreacted **1** (32%), 1-hydroxydiamantane (**12**, 52%), 4-hydroxydiamantane (**13**, 5%), and a mixture of dihydroxy diadamantanes (11%). MS (70 eV): *m*/*z* (%): 220 (22), 202 (100), 145 (20), 130 (24), 123 (25), 110 (18), 95 (29), 91 (33), 77 (26), 55 (20). Mass spectra and the retention times of **12** and **13** were identical to those for the standard samples obtained as described above.

Oxidation of 1 with *m*-chloroperbenzoic acid: *m*-Chloroperbenzoic acid (130 mg, 1.32 mmol) was added in one portion to a solution of **1** (90 mg, 0.48 mmol) in CH_2Cl_2 (25 mL). The reaction mixture was refluxed under stirring for 2 h, cooled to RT, filtered, and washed with aqueous Na_2SO_3, water, brine, and dried over Na_2SO_4. The GC–MS analysis of the reaction mixture indicated **1** (57%), 1-hydroxydiamantane (**12**, 23%), 4-hydroxydiamantane (**13**, 4%), and a mixture of dihydroxy diamantanes (6%) were present.

Oxidation of 1 with CrO_2Cl_2: Compound **1** (1.24 g, 6.59 mmol) was dissolved in CCl_4 (80 mL) and a solution of CrO_2Cl_2 (2.04 g, 13.2 mmol) in CCl_4 (20 mL) was added dropwise. The reaction mixture was kept at room temperature while stirring for 8 h. Then a saturated aqueous Na_2SO_3 solution was added (15 mL) and the mixture was shaken until the color changed from dark red to dark green. The organic layer was separated, the aqueous layer was extracted with $CHCl_3$ (3×10 mL). The organic extracts were combined, washed with water, then brine, and were dried over Na_2SO_4. The residue after solvent removal was separated by column chromatography on silica gel. Elution with pentane yielded unreacted **1** (470 mg, 2.50 mmol) and a 3:1 mixture of 1-chlorodiamantane (**20**) and 4-chlorodiamantane (**21**: 334 mg, 36.6% calculated on reacted **1**). The ^{1}H NMR spectra of **20** and **21** were identical to literature data.[45] 1-Chlorodiamantane (**20**): ^{13}C NMR (75 MHz, $CDCl_3$, 25°C, TMS): δ = 65.9, 49.5, 45.0, 40.9, 38.3, 37.17, 36.4, 33.4, 30.8, 25.1 ppm. 4-Chlorodiamantane (**21**): ^{13}C NMR (75 MHz, $CDCl_3$, 25°C, TMS): δ = 68.1, 48.1, 40.6, 36.9, 35.8, 25.3 ppm. After changing the eluent to pentane/diethyl ether = 4:1, 1-hydroxydiamantane (**12**: 387 mg, 46.3% calculated on reacted **1**) was isolated.

Reaction of 1 with Br_2 in CH_3CN: A mixture of **1** (95 mg, 0.51 mmol), CH_2Cl_2 (0.3 mL), CH_3CN (1 mL), and Br_2 (0.3 mL, 5.8 mmol) was stirred for 24 h at room temperature, quenched with Na_2SO_3 solution, and extracted with CH_2Cl_2 (3×5 mL). The combined extracts were washed with brine and dried over Na_2SO_4. The GC–MS analysis of the reaction mixture indicated 98% of 1-acetaminodiamantane (**22**) and 2% of 4-acetaminodiamantane (**23**). Column chromatography on silica gel (diethyl ether/methanol = 90:10) gave 1-acetaminodiamantane (**22**: 117 mg, 95%); spectroscopic data of the latter were identical to available data of the material described previously.[24] ^{1}H NMR (300 MHz, $CDCl_3$, 25°C, TMS): δ = 5.50 (br s, 1H), 2.22 (m, 2H), 2.03 (m, 2H), 1.93 (m, 4H), 1.90 (s, 4H), 1.45 (m, 8H), 1.49 ppm (m, 2H); ^{13}C NMR (75 MHz, $CDCl_3$, 25°C, TMS): δ = 169.1, 56.1, 41.5, 39.1, 38.7, 38.1, 37.3, 37.0, 32.8, 28.6, 25.1, 24.5 ppm; MS (70 eV): *m*/*z* (%): 245 (71), 230 (14), 202 (7), 186 (94), 171 (4), 157 (6), 143 (11), 130 (45), 129 (41), 95 (90), 94 (100), 79 (25), 67 (18), 53 (11). From the last fractions a mixture of **22** and **23** was isolated (9 mg). 4-Acetaminodiamantane (**23**): ^{13}C NMR (75 MHz, $CDCl_3$, 25°C, TMS): δ = 169.4, 50.8, 41.9, 38.7, 38.4, 36.4, 29.6, 24.4 ppm; MS (70 eV): *m*/*z* (%): 245 (100), 230 (6), 202 (10), 187 (46), 171 (3), 157 (3), 143 (10), 129 (45), 129 (8), 106 (44), 91 (20), 79 (25), 67 (12), 53 (9).

Oxidation of 1 with NO_2BF_4 in CH_3CN: A mixture of **1** (95 mg, 0.51 mmol), CH_2Cl_2 (0.3 mL), CH_3CN (1.5 mL), and NO_2BF_4 (0.6 g, 4.5 mmol) was stirred at room temperature for 0.5 h. Workup as above gave a mixture (GC–MS) of 1-acetaminodiamantane (**22**, 74%), 4-acetaminodiamantane (**23**, 22%), and diacetamides (4%). MS (70 eV): *m*/*z* (%): 302 (33), 287 (71), 243 (100), 228 (8), 201 (23), 186 (19), 163 (7), 148 (27), 129 (13), 106 (47), 94 (20), 77 (18), 60 (12).

Oxidation of 1 with HNO_3 in CH_3CN: A mixture of **1** (2.0 g, 10.6 mmol), $CHCl_3$ (6 mL), CH_3CN (25 mL), and 100% HNO_3 (17 mL, 0.4 mol) was stirred for 6 h at room temperature, poured onto ice, and extracted with $HCCl_3$ (3×10 mL). Extracts were washed with saturated Na_2CO_3 aqueous solution (5×5 mL), brine (2×10 mL), and then dried over Na_2SO_4. Column chromatography on silica gel (diethyl ether/methanol = 90:10) gave 1-acetaminodiamantane (**22**: 2.2 g, 84%), identical to the standard sample. Some product (ca. 0.3 g), together with 4-acetaminodiamantane (**23**) was found in the last fractions.

Photooxidation of 1 with TCB: A solution of diamantane **1** (200 mg, 1.06 mmol) and 1,2,4,5-tetracyanobenzene (75 mg, 0.42 mmol) in acetonitrile (160 mL) was irradiated with a low-pressure Hg-lamp in a quartz vessel for 1 h. Evaporation of the solvent and column chromatography on silica gel (cyclohexane/ethyl acetate = 7:2) gave diamantane **1** (128 mg, 0.68 mmol) and 2,4,5-tricyano-1-(4-diamantyl)benzene (**24**: 38 mg, 0.11 mmol, 10.5%) as a white solid, and unreacted TCB (45 mg, 0.25 mmol). 2,4,5-Tricyano-1-(4-diamantyl)benzene (**24**): M.p. 275 °C (decomp); ^{1}H NMR (300 MHz, $CDCl_3$, 25 °C, TMS): $\delta = 8.07$ (s, 1H), 7.90 (s, 1H), 2.12 (m, 6H), 2.02 (m, 3H), 1.82 (m, 4H), 1.80 ppm (m, 6H); ^{13}C NMR (75 MHz, $CDCl_3$, 25 °C, TMS): $\delta = 159.4$, 139.5, 132.4, 119.3, 116.7, 116.1, 114.5, 113.8, 113.6, 41.5, 37.6, 37.3, 37.1, 36.1, 25.4 ppm; MS (70 eV): *m*/*z* (%): 339 (100), 324 (7), 282 (5), 268 (4), 243 (21), 230 (9), 217 (4), 187 (6), 134 (3), 105 (9), 91 (19) 79 (18), 55 (11); elemental analysis calcd (%) for $C_{23}H_{21}N_3$ (339.4): C 81.38, H 6.24, N 12.38; found: C 81.61, H 6.53, N 12.21.

Acknowledgements

This work was supported by the Ukrainian Basic Research Foundation, the Deutsche Forschungsgemeinschaft, and the NATO Cooperative Science and Technology Research Program.

---

[1] P. von R. Schleyer, *J. Am. Chem. Soc.* **1957**, *79*, 3292–3292.

[2] C. Cupas, P. von R. Schleyer, D. J. Trecker, *J. Am. Chem. Soc.* **1965**, *87*, 917–918.

[3] T. M. Gund, V. Z. Williams, E. Osawa, P. von R. Schleyer, *Tetrahedron Lett.* **1970**, *11*, 3877–3880.

[4] V. Z. Williams, P. von R. Schleyer, G. J. Gleicher, L. B. Rodewald, *J. Am. Chem. Soc.* **1966**, *88*, 3862–3863.

[5] W. Burns, T. R. B. Mitchell, M. A. McKervey, J. J. Rooney, G. Ferguson, P. Roberts, *J. Chem. Soc. Chem. Commun.* **1976**, 893–895.

[6] W. Burns, M. A. McKervey, T. R. B. Mitchell, J. J. Rooney, *J. Am. Chem. Soc.* **1978**, *100*, 906–911.

[7] V. V. Danilenko, *Phys. Solid State* **2004**, *46*, 595–599.

[8] M. Azzi, D. Gully, M. Heaulme, A. Berod, D. Pelaprat, P. Kitabgi, R. Boigegrain, J.-P. Maffrand, G. LeFur, W. Rostene, *Eur. J. Pharmacol.* **1994**, *255*, 167–174.

[9] G. Skuza, Z. Rogoz, G. Quack, W. Danysz, *J. Neural Transm. Gen. Sect.* **1994**, *98*, 57–67.

[10] "Adamantane-Containing Polymers": L. J. Mathias, J. J. Jensen, V. R. Reichert, C. M. Lewis, G. Tullos in *Step-Growth Polymers for High-Performance Materials* (Eds.: J. L. Hedrick, J. W. Labadie), American Chemical Society, Washington, DC, **1996**, Series 624, Chapter 11.

[11] a) D. Ranganathan, V. Haridas, K. P. Madhusudanan, R. Roy, R. Nagaraj, G. B. John, M. B. Sukhaswami, *Angew. Chem.* **1996**, *108*, 1193–1195; *Angew. Chem. Int. Ed. Engl.* **1996**, *35*, 1105–1107; b) D. Ranganathan, V. Haridas, S. Kurur, R. Nagaraj, E. Bikshapathy, A. C. Kunwar, A. V. S. Sarma, M. Vairamani, *J. Org. Chem.* **2000**, *65*, 365–374.

[12] J. E. Dahl, S. G. Liu, R. M. K. Carlson, *Science* **2003**, *299*, 96–99.

[13] J. E. P. Dahl, J. M. Moldowan, T. M. Peakman, J. C. Clardy, E. Lobkovsky, M. M. Olmstead, P. W. May, T. J. Davis, J. W. Steeds, K. E. Peters, A. Pepper, A. Ekuan, R. M. K. Carlson, *Angew. Chem.* **2003**, *115*, 2086–2090; *Angew. Chem. Int. Ed.* **2003**, *42*, 2040–2044.

[14] H. Hopf, *Angew. Chem.* **2003**, *115*, 2046–2048; *Angew. Chem. Int. Ed.* **2003**, *42*, 2000–2002.

[15] a) R. C. Bingham, P. von R. Schleyer, *Fortschr. Chem. Forsch.* **1971**, *18*, 1–102; b) H. Hopf, *Classics in Hydrocarbon Chemistry*, Wiley-VCH, Weinheim, **2000**.

[16] a) R. C. Fort, *Adamantane: The Chemistry of Diamondoid Molecules*, Dekker, New York, **1976**; b) G. A. Olah, *The Chemistry of Cage Compounds*, Wiley, New York, **1990**.

[17] A. A. Fokin, P. R. Schreiner, *Chem. Rev.* **2002**, *102*, 1551–1593.

[18] G. A. Olah, *Angew. Chem.* **1995**, *107*, 1519–1532; *Angew. Chem. Int. Ed. Engl.* **1995**, *34*, 1393–1405.

[19] A. A. Fokin, P. R. Schreiner, P. A. Gunchenko, S. A. Peleshanko, T. E. Shubina, S. D. Isaev, P. V. Tarasenko, N. I. Kulik, H.-M. Schiebel, A. G. Yurchenko, *J. Am. Chem. Soc.* **2000**, *122*, 7317–7326.

[20] A. A. Fokin, T. E. Shubina, P. A. Gunchenko, S. D. Isaev, A. G. Yurchenko, P. R. Schreiner, *J. Am. Chem. Soc.* **2002**, *124*, 10718–10727.

[21] H. Stetter, C. Wulff, *Chem. Ber.* **1960**, *93*, 1366–1371.

[22] A. G. Yurchenko, N. I. Kulik, V. P. Kuchar, V. M. Djyakovskaya, V. F. Baklan, *Tetrahedron Lett.* **1986**, *27*, 1399–1402.

[23] I. K. Moiseev, P. G. Belyaev, N. V. Barabanov, O. P. Bardyug, E. H. Vishnevskii, N. I. Novatskaya, E. L. Golod, B. V. Gidaspov, *Zh. Org. Khim.* **1975**, *11*, 214–215.

[24] T. M. Gund, M. Nomura, P. von R. Schleyer, *J. Org. Chem.* **1974**, *39*, 2987–2994.

[25] F. Hollowood, A. Karim, M. A. McKervey, P. McSweeney, *J. Chem. Soc. Chem. Commun.* **1978**, 306–308.

[26] A. T. Balaban, P. von R. Schleyer, *Tetrahedron* **1978**, *34*, 3599–3609.

[27] S. Hala, S. Landa, V. Hanus, *Angew. Chem.* **1966**, *78*, 1060–1061; *Angew. Chem. Int. Ed. Engl.* **1966**, *5*, 1045–1046.

[28] A. de Meijere, S. Blechert, *Strain and Its Implications in Organic Chemistry, Vol. 273*, Kluwer Academic Publishers, Dordrecht, **1989**.

[29] A. A. Fokin, P. R. Schreiner, P. von R. Schleyer, P. A. Gunchenko, *J. Org. Chem.* **1998**, *63*, 6494–6502.

[30] P. von R. Schleyer, J. E. Williams, K. R. Blanchard, *J. Am. Chem. Soc.* **1970**, *92*, 2377–2386.

[31] T. Clark, T. M. O. Knox, M. A. McKervey, H. Mackle, J. J. Rooney, *J. Am. Chem. Soc.* **1979**, *101*, 2404–2410.

[32] G. A. Olah, A. Molnár, *Hydrocarbon Chemistry*, Wiley, New York, **1995**.

[33] M. Mella, M. Freccero, T. Soldi, E. Fasani, A. Albini, *J. Org. Chem.* **1996**, *61*, 1413–1422.

[34] E. Osawa, E. M. Engler, S. A. Godleski, Y. Inamoto, G. J. Kent, M. Kausch, P. von R. Schleyer, *J. Org. Chem.* **1980**, *45*, 984–991.

[35] M. Finn, R. Friedline, N. K. Suleman, C. J. Wohl, J. M. Tanko, *J. Am. Chem. Soc.* **2004**, *126*, 7578–7584.

[36] B. Kovac, L. Klasinc, *Croat. Chem. Acta* **1978**, *51*, 55.

[37] M. J. S. Dewar, S. D. Worley, *J. Chem. Phys.* **1969**, *50*, 654–667.

[38] A similar behavior was recently found by us for the D_{4h}-symmetric[4]rotane upon ionization: a) A. A. Fokin, P. R. Schreiner, S. I. Kozhushkov, K. Sattelmeyer, H. F. Schaefer III, A. de Meijere, *Org. Lett.* **2003**, *5*, 697–700; b) A. de Meijere, S. I. Kozhushkov, A. A. Fokin, I. Emme, S. Redlich, P. R. Schreiner, *Pure Appl. Chem.* **2003**, *75*, 549–562.

[39] A. A. Fokin, P. A. Gunchenko, S. A. Peleshanko, P. von R. Schleyer, P. R. Schreiner, *Eur. J. Org. Chem.* **1999**, 855–860.

[40] A. A. Fokin, B. A. Tkachenko, T. E. Shubina, P. A. Gunchenko, D. V. Gusev, J. K. Vohs, G. H. Robinson, A. G. Yurchenko, P. R. Schreiner, *Eur. J. Org. Chem.* **2002**, 3844–3849.

[41] T. E. Shubina, P. A. Gunchenko, A. G. Yurchenko, P. R. Schreiner, E. D. Butova, A. A. Fokin, *Theor. Exp. Chem.* **2002**, *38*, 8–14.

[42] W. Adam, A. Corma, M. A. Miranda, M.-J. Sabater-Picot, C. Sahin, *J. Am. Chem. Soc.* **1996**, *118*, 2380–2386.

[43] T. M. Gund, P. von R. Schleyer, G. D. Unruh, G. J. Gleicher, *J. Org. Chem.* **1974**, *39*, 2995–3003.

[44] D. E. Johnston, J. J. Rooney, M. A. McKervey, *J. Chem. Soc. Chem. Commun.* **1972**, 29–30.

[45] T. Courtney, D. E. Johnston, J. J. Rooney, M. A. McKervey, *J. Chem. Soc. Perkin Trans. 1* **1972**, 2691–2696.

[46] G. A. Olah, P. Ramaiah, C. B. Rao, G. Sandford, R. Golam, N. J. Trivedi, J. A. Olah, *J. Am. Chem. Soc.* **1993**, *115*, 7246–7249.

[47] R. Duddu, R. Damavarapu, *Synth. Commun.* **1996**, *26*, 3495–3501.

[48] S. R. Jones, J. M. Mellor, *J. Chem. Soc. Perkin Trans. 1* **1976**, 2576–2581.

[49] I. Tabushi, S. Kojo, P. von R. Schleyer, T. M. Gund, *J. Chem. Soc. Chem. Commun.* **1974**, 591.

[50] a) A. A. Fokin, P. R. Schreiner, *Adv. Synth. Catal.* **2003**, *345*, 1035–1052; b) P. R. Schreiner, A. A. Fokin, *Chem. Rec.* **2004**, *4*, 247–257.

[51] a) P. R. Schreiner, O. Lauenstein, E. D. Butova, P. A. Gunchenko, I. V. Kolomitsin, A. Wittkopp, G. Feder, A. A. Fokin, *Chem. Eur. J.* **2001**, *7*, 4996–5003; b) P. R. Schreiner, O. Lauenstein, E. D. Butova, A. A. Fokin, *Angew. Chem.* **1999**, *111*, 2956–2958; *Angew. Chem. Int. Ed.* **1999**, *38*, 2786–2788; c) P. R. Schreiner, O. Lauenstein, I. V. Kolomitsyn, S. Nadi, A. A. Fokin, *Angew. Chem.* **1998**, *110*, 1993–1995; *Angew. Chem. Int. Ed.* **1998**, *37*, 1895–1897.

[52] W. Adam, R. Curci, J. O. Edwards, *Acc. Chem. Res.* **1989**, *22*, 205–211.

[53] a) A. Bravo, H.-R. Bjorsvik, F. Fontana, F. Minisci, A. Serri, *J. Org. Chem.* **1996**, *61*, 9409–9416; b) A. Bravo, F. Fontana, F. Minisci, A. Serri, *Chem. Commun.* **1996**, 1843–1844.

[54] J. M. Mayer, *Acc. Chem. Res.* **1998**, *31*, 441–450.

[55] a) X. H. Du, K. N. Houk, *J. Org. Chem.* **1998**, *63*, 6480–6483; b) M. N. Glukhovtsev, C. Canepa, R. D. Bach, *J. Am. Chem. Soc.* **1998**, *120*, 10528–10533; c) A. A. Fokin, B. A. Tkachenko, O. I. Korshunov, P. A. Gunchenko, P. R. Schreiner, *J. Am. Chem. Soc.* **2001**, *123*, 11248–11252.

[56] B. A. Tkachenko, T. E. Shubina, D. V. Gusev, P. A. Gunchenko, A. G. Yurchenko, P. R. Schreiner, A. A. Fokin, *Theor. Exp. Chem.* **2003**, *39*, 90–95.

[57] a) G. A. Olah, H. C. Lin, *J. Am. Chem. Soc.* **1971**, *93*, 1259–1261; b) G. A. Olah, P. Ramaiah, *J. Org. Chem.* **1993**, *58*, 4639–4641; c) R. D. Bach, J. W. Holubka, R. C. Badger, S. J. Rajan, *J. Am. Chem. Soc.* **1979**, *101*, 4416–4417; d) I. K. Moiseev, Y. N. Klimochkin, M. N. Zemtsova, P. L. Trakhtenberg, *Zh. Org. Khim.* **1984**, *20*, 1435–1438.

[58] I. K. Moiseev, N. V. Makarova, M. N. Zemtsova, *Russ. Chem. Rev.* **1999**, *68*, 1002–1021.

[59] M. Mella, M. Freccero, A. Albini, *Tetrahedron* **1996**, *52*, 5533–5548.

[60] A. D. Becke, *J. Chem. Phys.* **1993**, *98*, 5648–5652.

[61] Geometry optimizations, frequency analysis of stationary points, and intrinsic reaction coordinate computations were carried with the Gaussian program package: Gaussian 03, Revision B.03, M. J. Frisch, G. W. Trucks, H. B. Schlegel, G. E. Scuseria, M. A. Robb, J. R. Cheeseman, J. A. Montgomery, Jr., T. Vreven, K. N. Kudin, J. C. Burant, J. M. Millam, S. S. Iyengar, J. Tomasi, V. Barone, B. Mennucci, M. Cossi, G. Scalmani, N. Rega, G. A. Petersson, H. Nakatsuji, M. Hada, M. Ehara, K. Toyota, R. Fukuda, J. Hasegawa, M. Ishida, T. Nakajima, Y. Honda, O. Kitao, H. Nakai, M. Klene, X. Li, J. E. Knox, H. P. Hratchian, J. B. Cross, V. Bakken, C. Adamo, J. Jaramillo, R. Gomperts, R. E. Stratmann, O. Yazyev, A. J. Austin, R. Cammi, C. Pomelli, J. W. Ochterski, P. Y. Ayala, K. Morokuma, G. A. Voth, P. Salvador, J. J. Dannenberg, V. G. Zakrzewski, S. Dapprich, A. D. Daniels, M. C. Strain, O. Farkas, D. K. Malick, A. D. Rabuck, K. Raghavachari, J. B. Foresman, J. V. Ortiz, Q. Cui, A. G. Baboul, S. Clifford, J. Cioslowski, B. B. Stefanov, G. Liu, A. Liashenko, P. Piskorz, I. Komaromi, R. L. Martin, D. J. Fox, T. Keith, M. A. Al-Laham, C. Y. Peng, A. Nanayakkara, M. Challacombe, P. M. W. Gill, B. Johnson, W. Chen, M. W. Wong, C. Gonzalez, J. A. Pople, Gaussian, Inc., Pittsburgh PA, **2003**.

[62] C. Gonzalez, H. B. Schlegel, *J. Phys. Chem.* **1990**, *94*, 5523–5527.

[63] V. V. Krishnamurthy, J. G. Shih, G. A. Olah, *J. Org. Chem.* **1985**, *50*, 1161–1164.

[64] H. Duddeck, F. Hollowood, A. Karim, M. A. McKervey, *J. Chem. Soc. Perkin Trans. 2* **1979**, 360–365.

Received: January 12, 2005
Revised: June 13, 2005